



ISSN: 2795-2215

Journal of Newviews in
Engineering & Technology
Faculty of Engineering
Rivers State University, Port Harcourt, Nigeria.

Email: rsujnet@gmail.com | Homepage: <https://rsujournal.com>



Design and Analysis of a Four-Step Distance Protection Scheme for the Afam-Port Harcourt 132kV Sub-Transmission Network.

Otonye E. Ojuka^{1,*}, Iwari G. Bala², Peace U. Sunday¹

¹Department of Electrical & Electronics Engineering, Rivers State University, PMB 5080 Port Harcourt, Nigeria.

²Department of Electrical & Electronics Engineering, Kenule Benson Saro-Wiwa Polytechnic, Bori, Rivers State.

*Corresponding Author: otonye.ojuka@ust.edu.ng

ARTICLE INFO	ABSTRACT
Article History Received: 5 April 2025 Received in revised form: 30 April 2025 Accepted: 2 May 2025 Available online: 28 May 2025	In electrical power systems, transmission lines are necessary for the conveyance of large amounts of power over great distances; however, their length makes it difficult to identify flaws. This article used the Afam-Port Harcourt 132 kV sub-transmission network as a case study to concentrate on the use of distance protection concepts for medium and long transmission lines. We performed a load flow study using ETAP tools and the Newton-Raphson approach to evaluate the system's current operating status. The study found that 17 of the 21 buses were critically undervoltage, with total active and reactive power losses of 40,030 kW and 115,534 kVAr, respectively. This shows how important it is to control voltage and lower power loss. On the high-voltage winding, seven power transformers were tapped. Shunt capacitor banks and on-load tap changers were used to control the voltage and lower the power loss, giving a total of 145,000 kVAr. A load flow analysis revealed improvements: all buses operated within safe voltage ranges; total active and reactive power losses decreased from 40,030 kW to 24,095.6 kW and from 115,534 kVAr to 61,446.5 kVAr, respectively. To determine the maximum and minimum fault current magnitudes at several system buses, a short-circuit study was carried out in line with the IEC 60909 standard. The lowest is 18.993 kA; the overall maximum fault current is indicated by the results as 186.681 kA. With zone 1 configured for instantaneous operation covering 80% of the line, zone 2 programmed to activate within 0.2 seconds for 100% of the line, zone 3 set to operate at 0.6 seconds for 120% of the line, and zone 4 designated to operate within 1 second for faults occurring in the reverse direction, we developed a four-step distance protection scheme. A three-phase fault was put on different parts of the line, and the relay sent out trip signals in the right places. This proved that the distance relay designs worked as planned.
Keywords Transmission, System, Load, Flow, Power, Loss, Mitigation, Shunt, Capacitors, Short-Circuit, Fault, Current, Voltage, Regulation, Winding.	

© 2025 Authors. All rights reserved.

1. Introduction

Safeguarding transmission lines is essential in modern power system networks to ensure

the safety of both equipment and humans involved in their operation. Transmission lines account for around 65% of power system problems, rendering them a primary focus for extensive examination and

innovation among researchers and designers in power system protection. According to Ojagh *et al.* (2014), in electrical networks, a significant concern is inadequate reliability and recurrent overloading, frequently stemming from deficient maintenance practices. These problems result in recurrent interruptions in the power supply. In high-voltage transmission systems, errors are more likely to arise in transmission lines than in power transformers and generators. We attribute this increased probability to the extended length of transmission lines and their susceptibility to external environments. Consequently, transmission lines require further protective measures compared to transformers and generators (Ojuga *et al.*, 2022).

Transmission cables frequently use distance relays for protection. They operate by determining the impedance between the relay and the fault site through local measurements of current and voltage. This approach relies on local measurements, with the relay reacting to the impedance between its terminal and the failure site. The primary categories of distance relays are impedance, admittance (or mho), and reactance distance relays. These relays can serve as either main or secondary protection. Understanding the functioning of distance relays is more complex than that of other relays due to the sophisticated principles and theories involved (Abdullah & Ahmed, 2019).

Distance relays can safeguard transmission cables by utilising various protection zones. These operational zones are crucial for preventing losses and technological damage caused by relay faults. Generally, we select these zones based on worst-case scenarios that encompass multiple factors affecting relay performance, thereby complicating the problem definition. Consequently, while designating operational zones, it is imperative to satisfy two fundamental

protection criteria: maintaining security without hindering coordination and attaining simultaneity (Ojagh *et al.*, 2014). Upon the occurrence of a fault, the relay transmits a signal to the circuit breaker, prompting the coils of the circuit breaker closest to the fault to become energised and automatically interrupt the circuit. Minimising the relay's operational period, in conjunction with transmission line protection, is essential to avert unwarranted tripping of circuit breakers linked to unaffected segments of the power system. Regarding protection procedures, protective devices are linked to monitor and isolate defective segments of the system. Their primary objective is to mitigate damage when problems arise. Disruptions in power continuity to a distribution feeder can complicate the re-energisation of the load without activating protective relays. This results from abnormally large inrush currents attributed to the loss of load diversity (Ojuga *et al.*, 2022).

These currents, primarily generated by transformers and motors, are transient and generally non-problematic. Nonetheless, motor starting currents can generate significant inrush currents, potentially triggering protective relay activation. Therefore, precautions are essential to avert relay malfunctions caused by inrush currents subsequent to power failures. Distance protection ideas are used to compare the impedance between where the relay is located and where the fault is located with a set threshold. The study concentrates on the Afam-Port Harcourt 132 kV sub-transmission network, with particular emphasis on the protection of feeder lines. Ko and So (2016) suggested a concept for the protection of extra-high voltage transmission lines employing distance protection. This model was validated through multiple testing, including fault detection scenarios such as single line to

ground (SLG), double line to ground (LLG), line to line (LL), and three-phase faults. These faults were generated at various locations to assess the model's performance. The results indicated the relay's precise functionality across diverse fault locations and categories.

Employing MATLAB/SIMULINK software helps facilitate the comprehension of the complexities associated with distant relays.

Zeya *et al.* (2021) performed a study on a two-step distance protection technique designed for flexible HVDC transmission lines. Through processing electrical characteristics, this study used low-pass filters with different cutoff frequencies to make the protection system work better and be more reliable. The simulations proved that the suggested distance protection system can quickly and accurately find metallic faults between poles and between poles and ground.

Akshay and Viranjay (2020) introduced a novel concept for feeder protection systems utilising the rapid switching characteristics of PhotoMOS solid-state relays. The results showed that using PhotoMOS devices instead of regular electromechanical relays greatly reduced the time it took to switch between operations.

Mohammad *et al.* (2018) suggested a new way to tell the difference between fault and non-fault events using the stacked parts of voltage signals in a two-dimensional decision plane. The suggested method takes into account both the rate of change in the magnitude of the voltage and its pattern of movement. This is done by keeping an eye on the movement of these superimposed magnitude components during the decision-making process. We evaluated the algorithm's performance across multiple power system events and compared it with established approaches. Findings show that the suggested method effectively tells the difference between stressed situations and

fault events during a range of power system disruptions, making remote relays much safer.

Marko *et al.* (2020) conducted a study on the application of a newly developed algorithm to identify fault spots within an electric power distribution radial feeder. This method uses an artificial neural network (ANN) to find broken lateral branches in the distribution network. The goal is to find the right feeder circuit breaker to turn off when a fault is found. The findings demonstrate that the algorithm accurately activates the circuit breakers across all fault conditions. Hashemi *et al.* (2014) introduced a novel methodology for backup distance protection designed for series-compensated transmission lines. This new method fixes problems with single-phase and double-phase to ground by using the inter-phase impedance instead of the positive-sequence impedance.

The results indicate that the proposed technique surpasses traditional distance protection strategies commonly employed in series-compensated transmission lines.

To accomplish the goal of the study, the following objectives were addressed.

- i. To model the electrical network from the data collected using the ETAP 2022 software.
- ii. To use the given parameters to perform load flow and short-circuit analysis on the Afam-Port Harcourt 132kV sub-transmission network to ascertain the existing state of the network.
- iii. To design a four-step distance protection scheme using the proposed methodology.
- iv. To validate the result through simulations on ETAP software.

2. Materials and Methods

2.1 Materials

The materials used in carrying out this research work are the single line diagram of Afam-Port Harcourt 132kV Sub-transmission network, Electrical Transient Analyser Program (ETAP) software, and a computer system. ETAP software was used to create a

digital twin of the power system network under investigation, while the per-unit system was used for all calculations. Table I contains transformer and lump load apparent power and voltage ratio ratings used for the power system design.

Table I: Equipment Data

S/N	Equipment ID	Capacity (MVA)	Voltage (kV)
1	T1	60	132/33
2	T2	60	132/33
3	T3	60	132/33
4	T4	40	132/33
5	T5	40	132/33
6	T6	30	132/33
7	T7	45	132/33
8	T8	60	132/33
9	T9	30	132/33
10	T10	60	132/33
11	T11	60	132/33
12	T12	40	132/33
13	T13	40	132/33
14	T14	40	132/33
15	T15	40	132/33
16	T16	60	132/33
17	T17	30	132/33
18	Lump 1	40.25	33
19	Lump 2	60	33
20	Lump 3	45.125	33
21	Lump 4	38.75	33
22	Lump 5	27.875	33
23	Lump 6	27.875	33
24	Lump 7	35	33

(Source: Transmission Company of Nigeria)

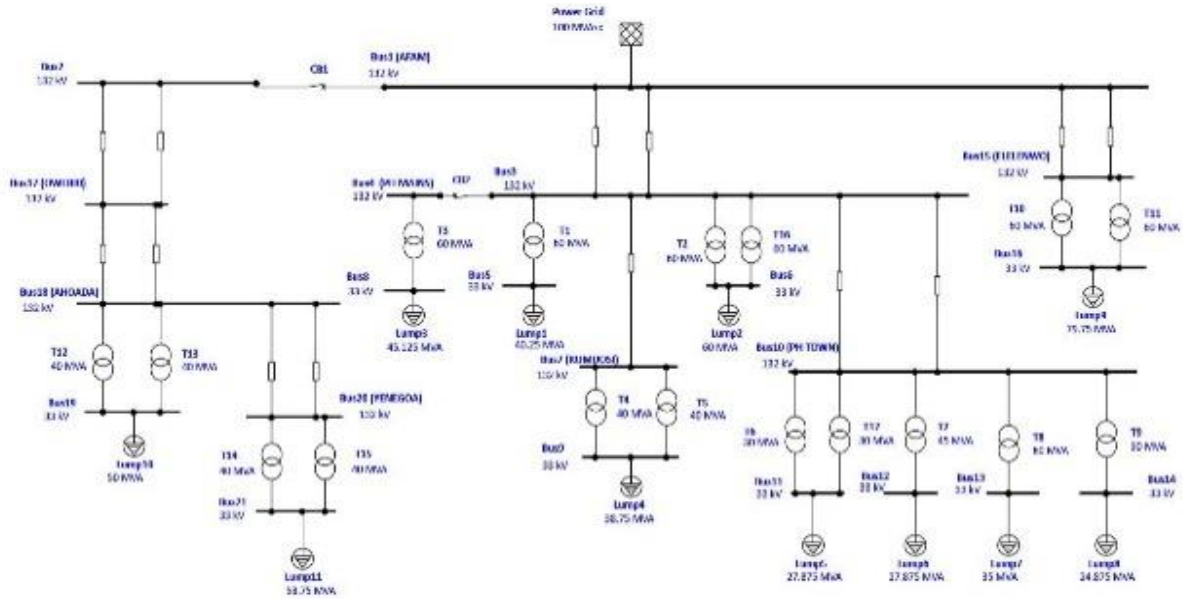


Figure 1: ETAP Representation of Afam-Port Harcourt 132kV Sub-Transmission Network

The Afam-Port Harcourt 132/33kV section, as displayed in Figure 1, comprises 17 transformers, 11 lump loads, 13 transmission lines and a power grid.

2.2 Methods

The method used for performing load flow analysis is known as Newton-Raphson's method of power flow analysis, while the IEC 60909 was used to perform short-circuit analysis as well as device duty calculations used for adequate ratings of switchgears. The protection scheme to be employed in this research work is a distance protection scheme using ETAP software for modelling and simulation.

2.2.1 Newton-Raphson Method

As usual load flow analysis will be conducted on the network under investigation to ascertain the voltage level, power flow and loss magnitude under balanced steady operating conditions using the conventional Newton Raphson (NR) solution algorithm. Thereafter, based on the findings, a novel

capacitor allotment and sizing algorithm will be deployed for system parameter optimisation for an efficient and reliable power supply.

The Newton-Raphson method is valid for power flow solutions and employed to solve the component of the Jacobian matrix in equation 1 (Ojuka & Ekwe, 2023).

$$\begin{bmatrix} \Delta P \\ \Delta Q \end{bmatrix} = \begin{bmatrix} J_1 & J_2 \\ J_3 & J_4 \end{bmatrix} \begin{bmatrix} \Delta \delta \\ \Delta V \end{bmatrix} \quad (1)$$

Where ΔP and ΔQ are the actual bus power and the operating force do not exactly match the vectors between the stated value and the calculated value, respectively; ΔV and $\Delta \delta$ represent the maximum power of the bus and angles in the form of additions; and J_1 to J_4 are called Jacobean matrices.

2.2.2 Short-Circuit Analysis

Short-circuit analysis provides a systematic mathematical approach used in determining the magnitude of fault currents (symmetrical and asymmetrical) at various locations in the power system, protective device withstand

and/or interrupting capability (device duty calculations), close and latch capability and to determine appropriate ratings or settings for relay coordination by calculating the maximum and minimum fault current at the buses. As earlier stated, the method used in calculating short-circuit magnitude is the per unit impedance method, while the standard used is per IEC 60909, which accounts for symmetrical and asymmetrical faults.

The procedure for short-circuit calculations includes:

- i. Prepare the single line diagram with equipment ratings, voltage level and impedance.
- ii. Convert the impedance value to a common base MVA.
- iii. Combine impedances.
- iv. Calculate short-circuit current at the fault location using equations 2 - 4.

Mathematically;

$$I_{sc} = \frac{\text{Fault MVA}}{\sqrt{3} \times kV} \quad (2)$$

But,

$$\frac{\text{Fault MVA}}{Z_{pu \text{ up to the point of fault}}} = \text{Base MVA} \quad (3)$$

Where;

I_{sc} = Short-circuit current

MVA = Rated power

Z_{pu} = per unit impedance

$$Z_{pu} = \frac{\text{Actual Impedance} \times \text{Base MVA}}{(\text{Base kV})^2} \quad (4)$$

2.2.3 Four-Stepped Distance Protection

According to Ojuka *et al.* (2022), switchgears separate a distance protection strategy into several steps or zones to make it easier to choose the right one during a breakdown. This research will delineate the distance protection method into four distinct steps or

zones.

The initial zone offers main protection to a transmission line and is often designed to encompass 80–90 percent of the line because of the inherent uncertainty regarding its real extent. There is a lot of doubt and uncertainty because of many factors, such as incorrect CT and PT ratios, DC offset in fault currents, changes in line parameters due to weather conditions, transient responses of capacitive voltage transformers, and not knowing how far the transmission line really goes. In this first zone, there is no deliberate delay in the operation of the switchgear; therefore, instantaneous protection is employed.

The second protective zone defends 10% of the unprotected line sections, besides 50% of the following line segment. This extended protection limits covers up 10% of the line parts that step one cannot protect, alongside safeguarding 50% of the adjacent line with its bus section should maximum underreach arise. The operation time is defined as follows due to the previous requirements:

The entire operation duration includes both step one execution and selective time distribution.

Where Selective time interval = CB operating time + Relay over-travel time

To avoid loss of selectivity, the second step should be set at half the shortest length when multiple lines exist adjacent to each other.

The third protective phase reaches into the system while back-up supporting the section under analysis as well as its adjacent line segment which amounts to 100% of the successive line section. This extended reach purpose is to deliver comprehensive backup safety for the next line section even when third-step maximum reach restrictions exist.

Each fourth category serves as complete back-up security for both previous zones by functioning ahead of their opposite direction. The installation reaches 100% of zone 3 to offer total backup protection within this section.

We must analyse phase a to phase b to phase c fault using Figure 2a as an illustration. The distance-measuring unit obtains positive sequence impedance values through analysing the problem using symmetrical components when it receives combined voltage and current measurements. A phase-to-phase fault leads to a parallel combination at the fault location of positive sequence networks with negative sequence networks, while zero-sequence networks operate in open-circuit configuration as shown in Figure 2b.

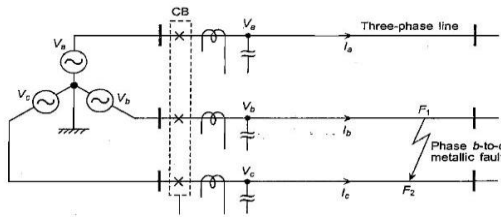


Figure 2a: Phase-b to Phase-c Fault

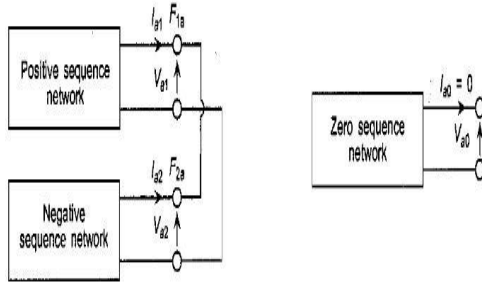


Figure 2b: Combination of Positive and Negative Sequence Network

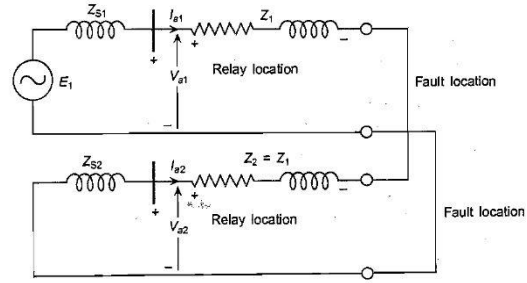


Figure 2c: Phase-a Sequence Network Connection for b-c Phase Fault

Applying KVL around the loop in Figure 2c, we have;

$$V_{a1} - I_{a1}Z_1 + I_{a2}Z_1 - V_{a2} = 0 \quad (5)$$

$$\text{Or } V_{a1} - V_{a2} = (I_{a1} - I_{a2})Z_1 \quad (6)$$

$$\text{Or } \frac{V_{a1} - V_{a2}}{I_{a1} - I_{a2}} = Z_1 \quad (7)$$

Therefore, the desired value for the positive sequence impedance between the relay location and fault point can be obtained by the ratio of the difference between positive and negative sequence voltages and currents. However, the sequence components of voltage and current are not readily available at the relay location, but the line voltages and currents are readily available thus, the sequence components can be obtained from the line voltages and currents using equations 8-15.

For the line voltages,

$$V_a = V_{a0} + V_{a1} + V_{a2} \quad (8)$$

$$V_b = V_{a0} + \alpha^2 V_{a1} + \alpha V_{a2} \quad (9)$$

$$V_c = V_{a0} + \alpha V_{a1} + \alpha^2 V_{a2} \quad (10)$$

From which we obtain;

$$V_b - V_c = (\alpha^2 - \alpha)V_{a1} + (\alpha - \alpha^2)V_{a2} \quad (11)$$

$$= (\alpha^2 - \alpha)V_{a1} - (\alpha^2 - \alpha)V_{a2}$$

$$= (\alpha^2 - \alpha)(V_{a1} - V_{a2}) \quad (12)$$

$$\text{Thus, } V_{a1} - V_{a2} = \frac{V_b - V_c}{\alpha^2 - \alpha} \quad (13)$$

Similarly, for line currents

$$I_{a1} - I_{a2} = \frac{I_b - I_c}{\alpha^2 - \alpha} \quad (14)$$

$$\text{Therefore, } \frac{V_{a1} - V_{a2}}{I_{a1} - I_{a2}} = \frac{V_b - V_c}{I_b - I_c} = Z_1 \quad (15)$$

Thus, to determine the positive sequence impedance up to fault point Z_1 , in a case of phase b-to-c faults, a distance measuring unit with voltage of $(V_b - V_c = V_{bc})$ and current of $(I_b - I_c)$ will be required. Similarly, in order to determine the positive sequence

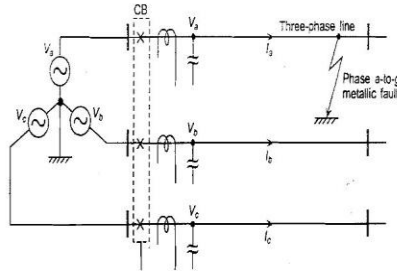


Figure 3(a) Phase a-to-g metallic fault

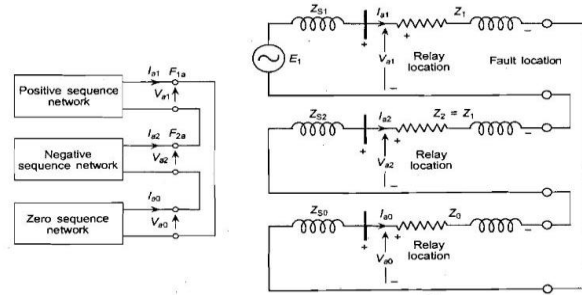


Figure 3(b) Equivalent circuit of Phase-a Sequence Network Connections for a-g Fault

Applying KVL around the loop in Figure 3(b), birthed equations (17-24);

$$V_{a0} + V_{a1} + V_{a2} = I_{a1}Z_1 + I_{a2}Z_1 + I_{a0}Z_0 \quad (16)$$

Recalling equation (8), $V_a = V_{a0} + V_{a1} + V_{a2}$

Adding and subtracting $I_{a0}Z_1$ on the right-hand side, we have;

$$V_a = I_{a1}Z_1 + I_{a2}Z_1 + I_{a0}Z_0 - I_{a0}Z_1 + I_{a0}Z_0 \quad (17)$$

$$V_a = Z_1(I_{a1} + I_{a2} + I_{a0}) + I_{a0}(Z_0 - Z_1) \quad (18)$$

impedance for phase a-to-b and c-to-a faults, two more distance measuring units with inputs of V_{ab} , $(I_a - I_b)$ and V_{ca} , $(I_c - I_a)$ will be required. These distance measuring units are known as phase fault units.

For ground faults, they are usually represented by a series connection of the positive, negative and the zero-sequence equivalent circuit as shown in Figure 3(b).

$$V_a = I_a Z_1 + I_{a0}(Z_0 - Z_1) \quad (19)$$

Or

$$V_a = Z_1 \left(I_a + \frac{Z_0 - Z_1}{Z_1} I_{a0} \right) \quad (20)$$

However,

$$I_{a0} = \frac{I_a + I_b + I_c}{3} \quad (21)$$

Let $I_a + I_b + I_c = I_{res}$

Where I_{res} is the residual current

$$\text{Therefore, } I_{a0} = \frac{I_{res}}{3} \quad (22)$$

$$\text{Hence, } V_a = Z_1 \left(I_a + \frac{Z_0 - Z_1}{Z_1} I_{res} \right) \quad (23)$$

Finally, we obtain the desired impedance as the ratio of:

$$Z_1 = \frac{V_a}{I_a + \frac{Z_0 - Z_1}{3Z_1} I_{res}} \quad (24)$$

In the above equation (24), Z_1 appears on both sides and the expression appears a bit mixed up. However, in actual practice, there is a definite relationship between Z_0 and Z_1 . For three-phase transmission lines, Z_0 is 2.5 to 3 times Z_1 . The exact relationship depends on the geometry of the phase conductors and the placement of earth conductors. Assuming $Z_0 = 3 Z_1$, triggers the transformation of equation (24) into equations (25 and 26).

$$Z_1 = \frac{V_a}{I_a + \frac{2}{3} I_{res}} \quad (25)$$

$$= \frac{V_a}{I_a + KI_{res}} \quad (26)$$

$$\text{where } K = \frac{Z_0 - Z_1}{3Z_1}$$

Thus, the phase current has to be compensated with a fraction of the residual current I_{res} . The factor K is known as the residual current compensation factor or zero-sequence compensation factor. Therefore, three numbers of distance measuring units with inputs of $[V_a, (I_a + KI_{res})]$, $[V_b, (I_b + KI_{res})]$ and $[V_c, (I_c + KI_{res})]$ will be required to accommodate all

three single-line to ground faults. These distance measuring units are known as ground fault units.

3. Results and Discussion

The results obtained after carrying out a load flow analysis, ensuring voltage regulation and power loss minimisation, carrying out a short-circuit analysis, and designing a four-step distance protection scheme on the Afam-Port Harcourt 132kV Sub-Transmission Network.

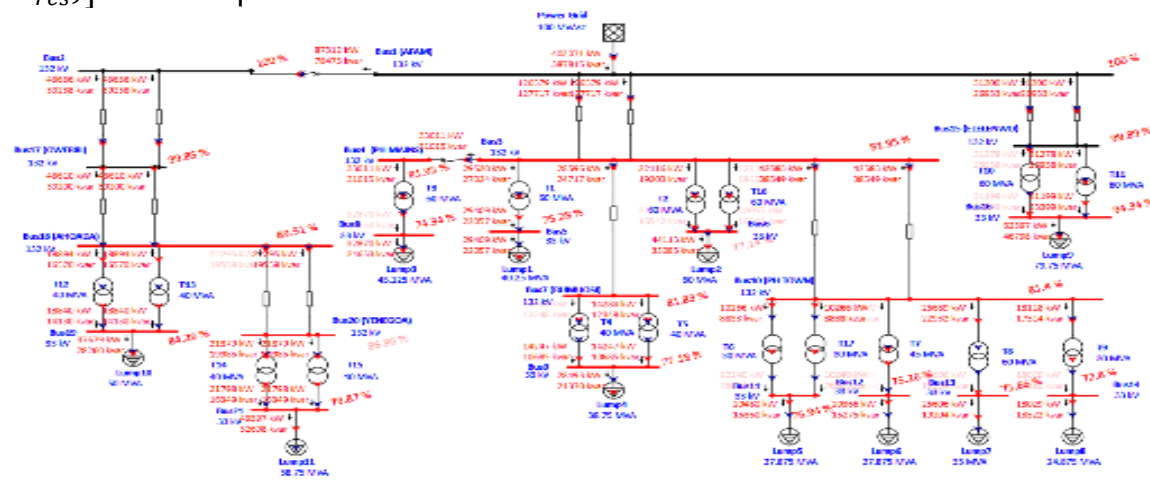


Figure 4: Existing Load Flow Result for Afam-Port Harcourt 132kV Sub-Transmission Network

We determined the current operational status of the equipment in the power system network by conducting a load flow study. Figure 4 shows a visual representation of the results. The results indicated that 17 of the 21 buses were marked red by the ETAP software due to a critical under-voltage condition, failing to operate within the IEEE permissible voltage limit of $\pm 5\%$. Therefore, implementing a voltage regulation scheme is essential. The overall active and reactive power losses in the system are 40,030.0 kW and 115,534.0 kVar, respectively.

3.1 Improvement of Afam-Port Harcourt 132kV Sub-Transmission Network

From the results obtained after performing a load flow analysis on the existing network, it is observed that the network is operating in a critical state, thus, it is pertinent to proffer methods for improvement. In this section, shunt capacitors and transformer tap changers will be employed for voltage regulation and power loss mitigation. The results obtained are elaborately discussed in this section.

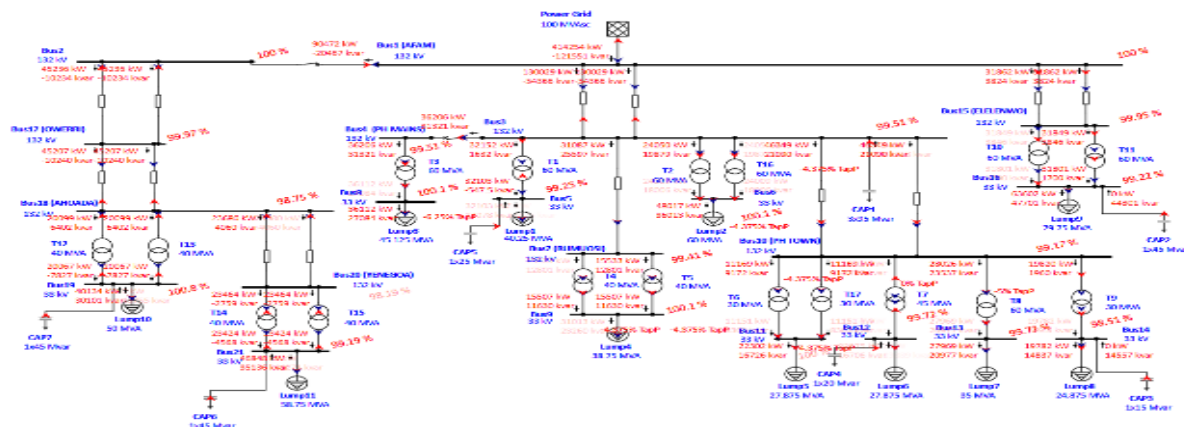


Figure 5: Load Flow Result of Afam-Port Harcourt 132kv Sub-Transmission Network after Improvement

After the transformer taps were adjusted and shunt capacitor banks were put in place, a load flow analysis was done to check how well the power system network was working again. Unlike Figure 4, Figure 5 shows no red-marked bus, indicating that all buses are operating within acceptable voltage limits. Additionally, the overall active power loss

decreased from 40,030.0 kW to 24,095.6 kW, while the total reactive power loss diminished from 115,534.0 kVar to 61,446.5 kVar.

3.3 Short Circuit Analysis of Afam-Port Harcourt 132kV Sub-Transmission Network

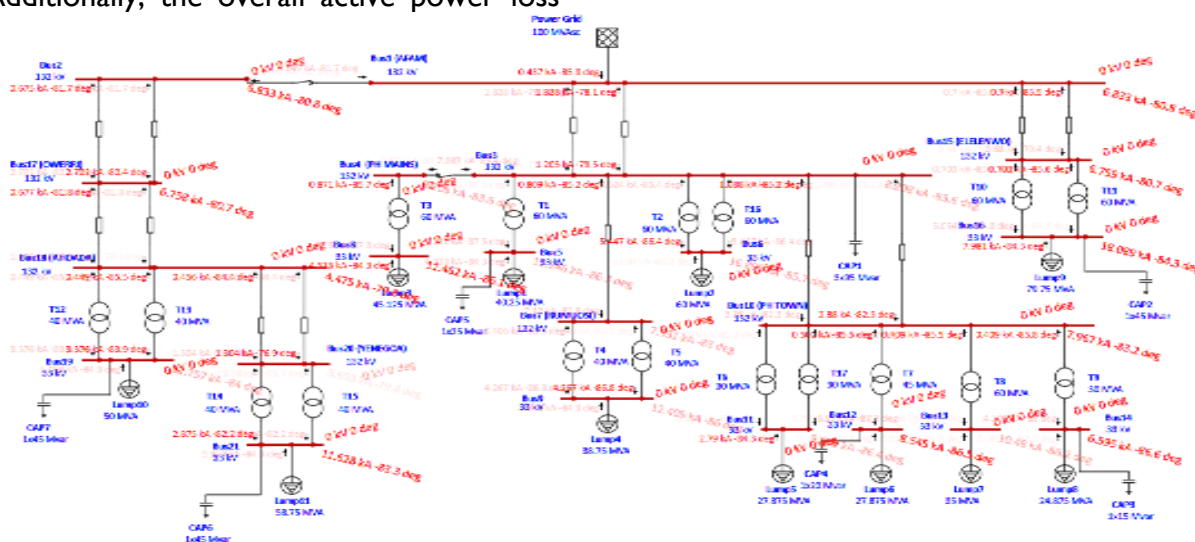


Figure 6: Maximum Short-Circuit Analysis of Afam-Port Harcourt 132kV Sub-Transmission Network

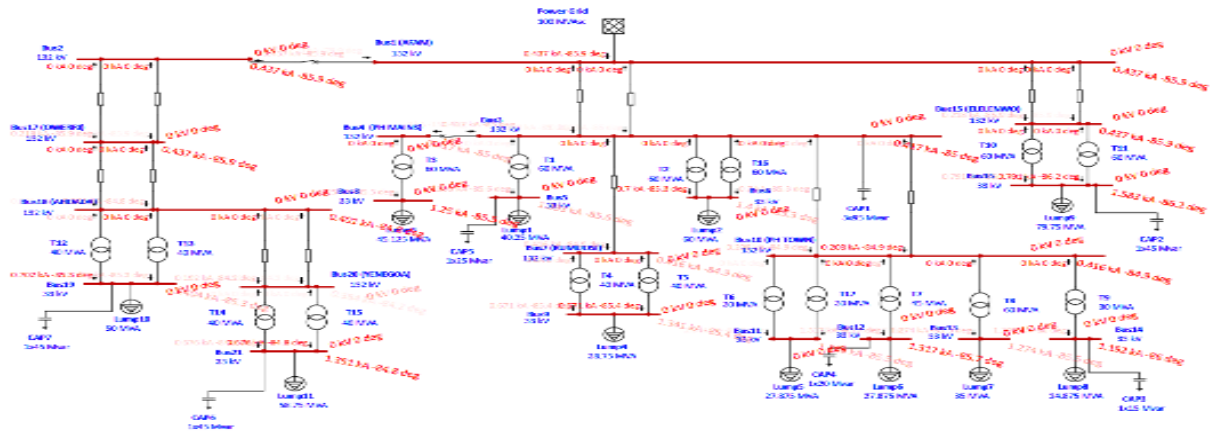


Figure 7 Minimum Short-Circuit Analysis of Afam-Port Harcourt 132kV Sub-Transmission Network

As earlier stated, a short-circuit analysis is crucial for determining the magnitude of fault current at various locations, which will aid adequate ratings of switchgears (circuit breakers and protective relays). Thus, Figures 6 and 7 show a pictorial view of the result obtained after carrying out a short-circuit analysis on the power system network under investigation. The magnitudes of voltage and fault current at various locations are displayed in kV and kA respectively.

3.3 Design of a Four-Stepped Distance Protection Scheme

A four-step distance protection scheme was designed for Line 10. The first step or zone covers 80% of the transmission line in a forward direction, the second step or zone covers 100% of the line in a forward direction, the third step or zone was designed to cover 120% of the line in a forward direction, and the fourth step or zone was designed to cover 50% of the line in a reverse direction. Furthermore, zone 1 was set to operate instantaneously, zone 2 was set to operate in 0.2 seconds, zone 3 was set to operate in 0.6sec, and zone 4 was set to operate in 1 second. The results obtained are displayed and explained in this section.

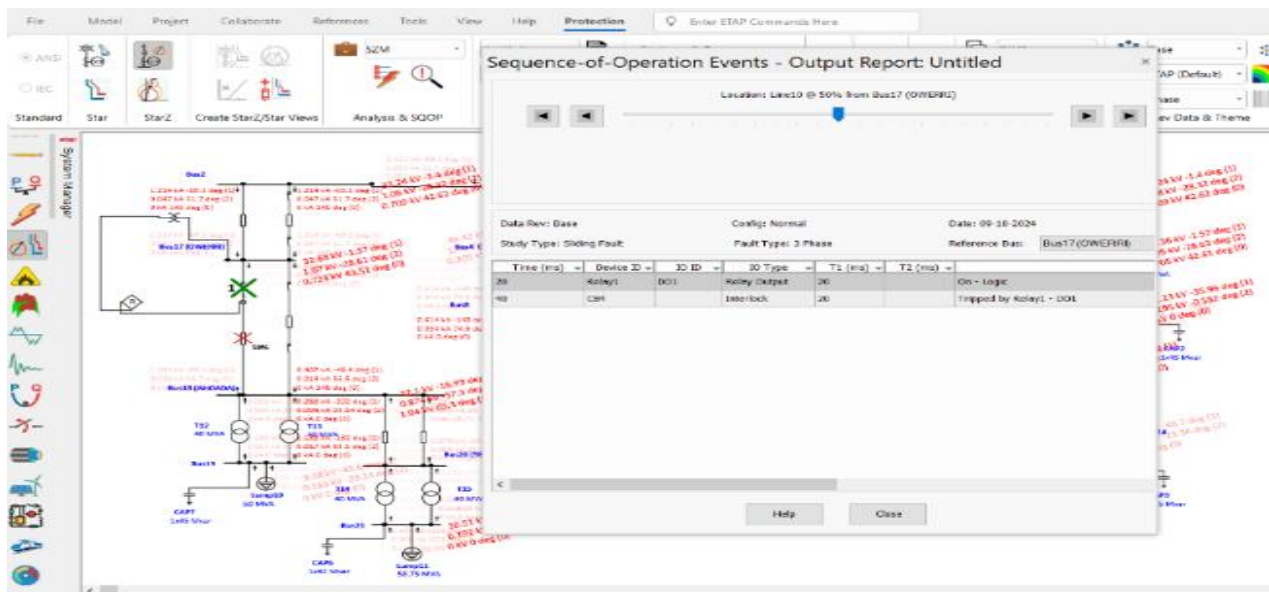


Figure 8: Fault at 50% of Line 10

A three-phase fault was inserted at 50% of the line in order to verify the effectiveness of the protection scheme designed and a pictorial view of the result is displayed in Figure 8. From the results displayed in the sequence of operation section, the tripping time of the relay and circuit breaker is shown to be 20ms each. However, since the fault is at 50% of the line, it is still in zone I, thus, expected to trip instantaneously (no

intentional delay). Therefore, the total time required to issue a trip signal in zone I is the operating time of the relay + the operating time of the circuit breaker. The magnitudes of current and voltage in the positive, negative, and zero sequences are displayed in kA and kV respectively.

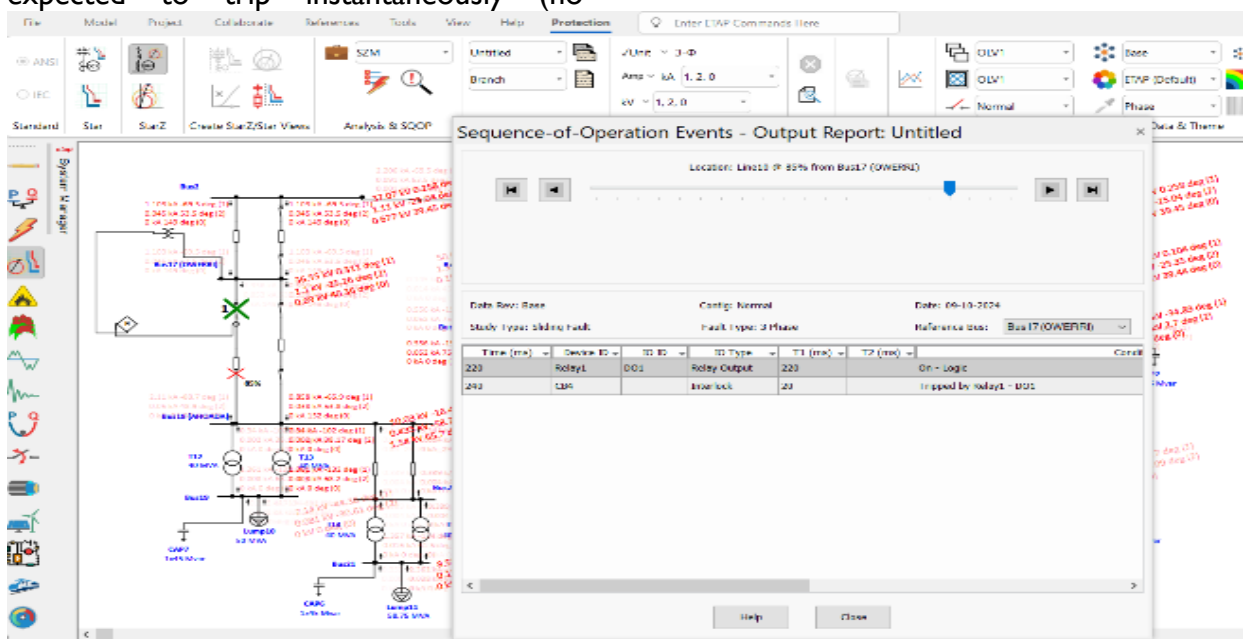


Figure 9: Fault at 85% of Line 10

In order to verify the effectiveness of zone 2 protection, a fault was inserted at 85% of the transmission line, and the result is displayed in Figure 9. From the result displayed, it is evident that the fault was isolated by zone 2 protection as it can be seen from the time of operation of the relay. Zone 2 was set to

operate at 0.2 sec for 100% of the line section, and the relay operating time is 20 ms, thus, the total time of operation for the relay should be 220 ms as displayed in Figure 9. Therefore, this validates the effectiveness of zone 2 protection.

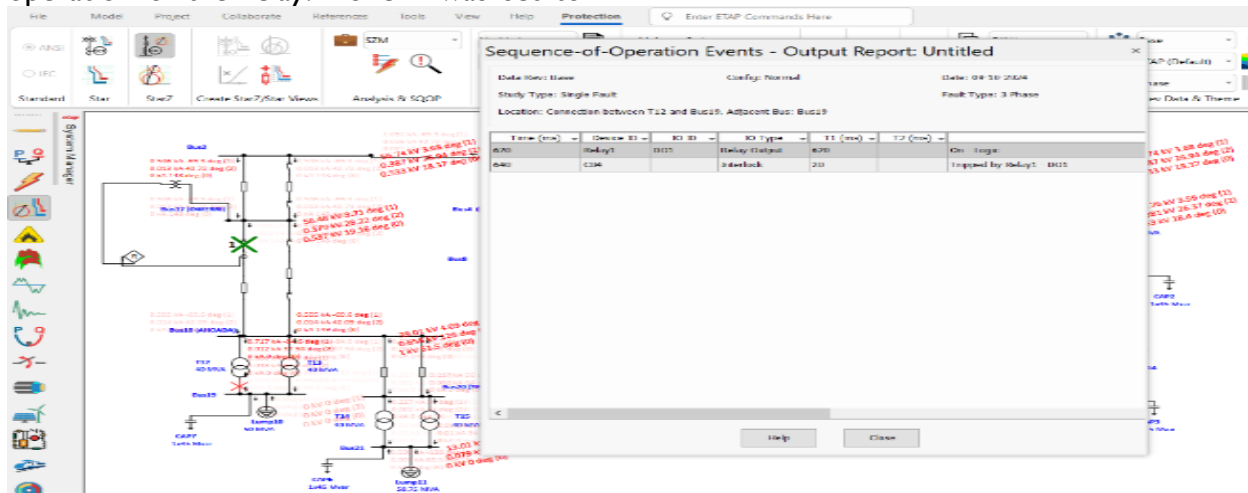


Figure 10: Fault at 120% of the Line

Zone 2 covers 100% of the line, thus, its jurisdiction ends at the transformer, while zone 3 covers 120% of the line, thus, it should be able to detect a fault after the transformer. Figure 10 displays the result obtained after inserting a fault after the

transformer (T12), and the effectiveness of zone 3 is evident from the tripping time displayed in the sequence of operation. Zone 3 was set to operate at 0.6sec, and the operating time of the relay is 20ms. Thus, the total operating time of the relay is 620ms.

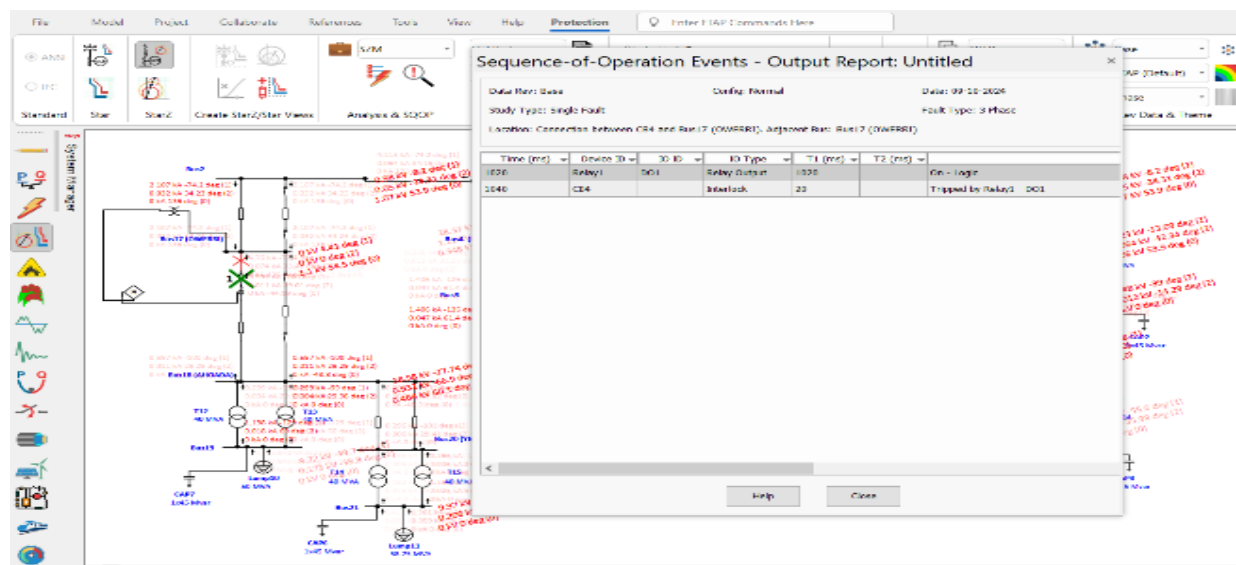


Figure 11: Fault in the Reverse Direction

As earlier stated, zone 4 was configured to operate at 1sec when a fault occurs in the reverse direction. Thus, a fault was inserted in order to verify the effectiveness of zone 4 and the result obtained is displayed in Figure 11. From the result obtained, it is also evident from the tripping time that it is a zone 4 operation. The total time of operation of the relay is 1020ms which is a combination of the zone operating time and the relay operating time. Therefore, this validates the effectiveness of the distance protection scheme.

4. Conclusions

This paper proposes a methodology for safeguarding extensive transmission lines through distance protection principles, utilizing the Afam-Port Harcourt 132 kV sub-transmission network as a case study. We modelled and analysed the power system network under examination using the Electrical Transient Analyzer Program (ETAP) software.

The software's load flow analysis of the power system network showed that 17 of the 21 buses were marked red. This means that these buses are working under critical low voltage conditions, which is different from the IEEE $\pm 5\%$ voltage regulation standard. Moreover, the cumulative active and reactive power losses produced by branch elements in the power system amounted to 40,030 kW and 115,534 kVAr, respectively. Therefore, it was essential to utilise a method for reactive power compensation to regulate voltage and minimise power loss.

To keep the voltage stable and cut down on power losses, capacitor banks with a total of 480,000 kVAr were installed at seven buses to provide reactive power compensation. On-load tap changers were also used to change the taps on the high-voltage windings of seven power transformers.

We conducted a load flow analysis to evaluate the system's operational status following the improvements. The results showed that all buses worked within the IEEE allowed voltage limits. At the same time, the active and reactive power losses from branch elements went down from 40,030 kW to 24,095.6 kW and from 115,534 kVAr to 61,446.5 kVAr.

According to the IEC 60909 standard, a short-circuit analysis of the power system network was done to find the highest and lowest fault current levels in different parts of the system. The maximum fault current magnitude at the bus is 186.681 kA, while the minimum fault current magnitude is 18.993 kA.

A four-step distance protection scheme was developed, with zone 1 designed to operate instantaneously for 80% of the line section in the forward direction, zone 2 to activate within 0.2 seconds for 100% of the line section in the forward direction, zone 3 to function at 120% of the line in the forward direction, and zone 4 configured to operate for faults in the reverse direction. We evaluated the efficacy of the protection scheme by simulating a fault at different segments of the transmission line using ETAP software. The findings demonstrated the proper functioning of the protective relay; hence, they substantiated the suggested methodology for distance protection.

Following the adjustment of transformer taps and the installation of shunt capacitor banks, a load flow analysis was conducted to confirm the operational status of the examined power system network. Unlike Figure 4, Figure 5 shows no red-marked bus, indicating that all buses are operating within acceptable voltage parameters. Additionally, the overall active power loss decreased from 40,030.0 kW to 24,095.6 kW, while the total reactive power loss diminished from 115,534.0 kVAr to 61,446.5 kVAr.

5. Recommendations

During this research work, some observations were made which led to the following recommendations:

- i. The existing state of the network is critical and requires voltage improvement at the downstream, thus, the developed model should be used as an important component in power system network planning and optimisation.
- ii. The research work should be further extended to cover other power system domains, such as the generation part of the network.
- iii. It should also be extended to include other protection schemes such as a conjunction of distance and over-current relays for

transmission line protection for comparative purposes to observe the effects and determine the best protective scheme to be employed for transmission line protection.

Acknowledgements

Authors are very grateful to all those who supported this research in the form of financial assistance and/or provision of the necessary resources.

References

- Abdullah H. A. & Ahmed J. S. (2019), A new approach of Mho distance relay for Transmission line protection. *Institute of Physics (IOP) Conference Series: 2nd International Conference on Sustainable Engineering Techniques (ICSET 2019)*. Pp. 1-15.
- Akshay, K., & Viranjay, M., S. (2020). A novel feeder protection system using fast switching photomos relay. *2020 11th International Conference on Computing, Communication and Networking Technologies (ICCCNT)*, 1-4, 2020.
- Hashemi S. M., Tarafdar H. M. & Seyedi H. (2014), A Novel Backup Distance Protection Scheme for Series-Compensated Transmission Lines. *IEEE Transactions on Power Delivery*, 29(2), 699-707.
- Ko K., A. & Soe S., E., A. (2016), Protection of Extra High Voltage Transmission Line Using Distance Protection. *International Journal for Innovative Research in Multidisciplinary Field*, 2(11), 477-485.
- Marko, I., Stjepan, S., Juraj, H., & Ante M. (2020). Study of a centralised radial feeder protection in electric power distribution using artificial neural networks. *Sustainable Energy, Grids and Networks* 22, 100331, 2020.
- Mohammad S. P., Majid S.-P., Peyman J. (2018), A blocking scheme for enhancement of distance relay security under stressed system conditions. *Elsevier; Electrical Power and Energy Systems* 94, 104-115.
- Ojaghi M, Mazlumi K, Azari M (2014), Zone-3 Impadance Reach Setting of Distance Relays by Including In-feed Current Effects in an Adaptive Scheme. *International Journal of Engineering*, 27(7), 1051-1060.
- Ojuka O. E., Ekwe J. P. & Sunday P. U. (2022), Design of Distance Protection Scheme for an 11kv Distribution Feeder. *Journal of Recent Trends in Electrical Power System*, 5(13), 1-17.
- Ojuka, O., E., & Ekwe, J., P. (2023). Voltage Regulation and Power Loss Reduction using Optimal Capacitor Placement in Distribution System. *Journal of Recent Trends in Electrical Power System*, 6(1), 12-27.
- Vijay H. M. & Bhavesh R. B. (2016), *Energy Systems in Electrical Engineering*. Springer, DOI 10.1007/978-981-10-1572-4.
- Zeya F., Minghao W., Junchao Z. & Minghao W. (2021), A Novel Two-step Distance Protection for Flexible HVDC Transmission Lines. *2021 International Conference on Power System and Energy Internet (PoSEI2021)*, 256, 6-12.